Pan-Arctic 200m Resolution Ice Concentration Mapping by Fusing RCM, Sentinel-1 and AMSR2 Data via Deep Learning

Mabel Heffring [a], Lincoln Linlin Xu [a]*

[a] *Department of Geomatics Engineering, University of Calgary, Alberta, Canada 1st Author – mabel.heffring1@ucalgary.ca, 2nd Author – lincoln.xu@ucalgary.ca*

* Corresponding author

Keywords: Pan-Arctic Ice Mapping, Data Fusion, Deep Learning

Abstract:

Accurate, timely and consistent mapping of Arctic sea ice distribution and change is essential for climate change studies, Arctic sea route navigation and the climate adaptation of the people and animals that call the Arctic home. Every day, a large amount of satellite images are collected by active and passive remote sensing systems over the Pan-Arctic region, including (a) Synthetic Aperture Radar (SAR) from the RADARSAT Constellation Mission (RCM) and Sentinel-1, and (b) Passive Microwave (PM) radiometry from the Advanced Microwave Scanning Radiometer 2 (AMSR2). Integrating these data sources using cutting-edge deep learning methods can improve daily Pan-Arctic sea ice concentration (IC) estimation to better support various critical Arctic applications.

Although SAR systems enable high-resolution ice mapping due to their fine spatial resolution, they do not provide complete daily Pan-Arctic coverage and have strong noise patterns (particularly in open-water areas), e.g., incidence angle noise and thermal noise. PM systems, despite having low spatial resolution, provide complete daily Pan-Arctic coverage with clear delineation between ice and open water. Various data fusion methods have been developed to combine the strengths of both systems for sea ice mapping. Wang et al. (2016) proposed a data assimilation method where labelled SAR and PM data are combined in a Bayesian framework to generate improved IC estimation. Deep learning methods, such as Convolutional Neural Networks (CNN), have been demonstrated as effective for merging these datasets without the need for pixel-level data labels (Malmgren-Hansen et al., 2021; Wulf et al., 2024). However, integrating Sentinel-1, RCM and PM data using advanced deep learning models for Pan-Arctic sea IC mapping is still an insufficiently researched issue. We propose a transformer-based architecture that achieves high-resolution Pan-Arctic IC product by improving the spatial resolution of PM IC product using Sentinel-1, RCM, and AMSR2 89.0GHz images.

The first contribution of this research is the development of a new high-resolution transformer architecture, which can better preserve small ice features, e.g., lead/cracks, ice edges and ice floes. The transformer model is independently trained on three higher resolution datasets: RCM SAR, Sentinel-1 SAR, and 89.0GHz AMSR2. The SAR models are trained using the corresponding horizontal transmit-receive (HH) and horizontal transmit-vertical receive (HV) channels, along with a cross-correlation layer between the two dual-polarized channels. This cross-correlation highlights physical structures present in both channels, while minimizing the impact of noise patterns. The AMSR2 model is trained using 89.0H and 89.0V channels, which are the highest resolution among the AMSR2 dataset and can provide information about small ice features when SAR data is not available. The SAR models output 200m IC maps, whereas the AMSR2 model outputs 3km-by-5km IC map.

The second contribution of this research is the design of a geographically-weighted L1 loss function that better address the uncertainties in the reference IC data. The PM IC product, which is derived by using the NASA Team (NT) algorithm, is used as reference in this research. This NT algorithm is a widely used approach to generate coarse-resolution IC product using AMSR2 data (Cavalieri et al., 1984). The NT product achieves better performance for open water region and ice region than the marginal ice zone (MIZ) region. Therefore, to leverage the spatially-varying nature of product uncertainty, we design a geographically-weighted loss function approach according to the U.S. National Ice Center daily ice charts, where we assign the highest weight to open water region, medium weight to the ice region, and lowest weight to the MIZ region. Furthermore, the L1 loss is used to calculate the discrepancies between 11 reference IC classes and the model output. The L1 loss is less sensitive to outliers/errors in the reference IC than the commonly adopted L2 loss, which reduces the effect of ambiguity on the model. The combined use of the geographically-weighted approach and the L1 loss leads to a new solution that can better address the uncertainties in the coarse-resolution NT

https://doi.org/10.5194/ica-abs-10-105-2025

product. RCM, Sentinel-1, and 89.0GHz AMSR2 data from September 2021 are used to train and validate the models, with 7 dates for training and 3 dates for validation. Each dataset is split into 256x256 image samples, and each model is trained for 50 epochs. Table 1 summarizes the validation L1 loss and epoch at the point of convergence for each model.

Pan-sharpening Dataset	Training samples	Validation samples	Validation L1 Loss
Sentinel-1	40,064	17,622	4.0504 e-05 (epoch 29)
RCM	37,721	20,304	4.0843 e-05 (epoch 36)
89.0GHz AMSR2	71,364	30,586	3.1404 e-05 (epoch 48)

Table 1. Model Validation Results

The third contribution of this research is an operational Pan-Arctic IC mapping solution by fusing Sentinel-1, RCM, NT product, and AMSR2 high-resolution channel (i.e., 89.0GHz channel). Our system merges four different products generated by our algorithms, i.e., (1) a 200m resolution Sentienl-1 IC map, (2) a 200m RCM IC map, (3) a 3km-by-5km 89.0GHz IC map, as well as (4) the NT 25km-by-25km IC map. The fusion approach considers the different uncertainty levels and the spatial resolution of different products. We design a new weather mask using the 18.7GHz and 89.0GHz AMSR2 channels to better remove the influence of clouds and precipitation. The final Pan-Arctic map generated by our system is evaluated with the EUMETSAT OSI SAF sea IC product, and it indicates that our product achieved an R2 score of 0.82. Figure 1 illustrates the IC mosaic and corresponding regions of interest for September 4th 2021.

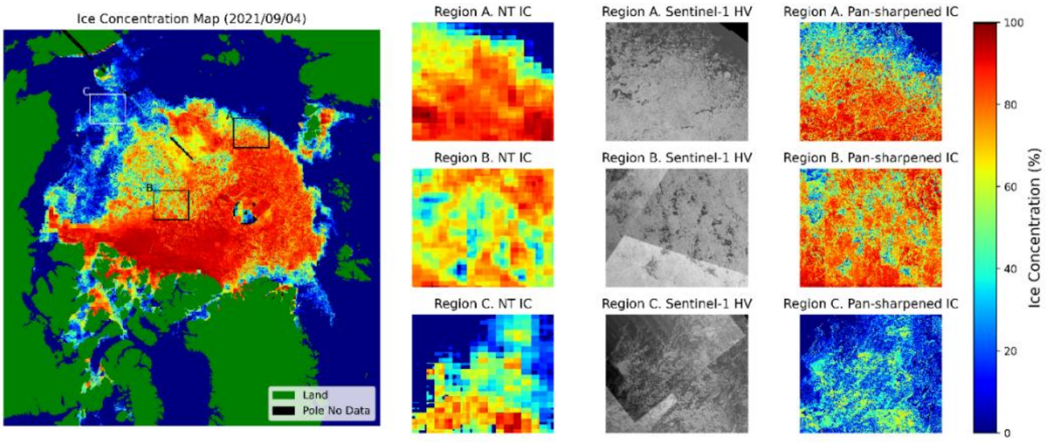

Figure 1. Pan-Arctic Ice Concentration Map achieved by our system for September 4th, 2021. The rightmost column shows our results, which offer much more details than the NT IC products, and demonstrates visual consistency with Sentinel-1 images.

Accurate daily Pan-Arctic sea ice mapping is crucial for monitoring climate change, supporting Northern Indigenous communities, and ensuring safe navigation as sea ice extents continue to decrease. Overall, the novel deep learning based data fusion approach proposed in this abstract can generate daily Pan-Arctic 200m resolution IC product, and has the potential to support long-term, continuous mapping of Pan-Arctic sea ice, providing a reliable baseline for future environmental studies of the Arctic and cryosphere.

References

Cavalieri, D. J., P. Gloersen, and W. J. Campbell., 1984. Determination of sea ice parameters with the Nimbus 7 SMMR. *J. Geophys. Res.*, 89, pp.5355-5369.

Malmgren-Hansen, D., Pedersen, L.T., Nielsen, A.A., Kreiner, M.B., Saldo, R., Skriver, H., Lavelle, J., Buus-Hinkler, J. and Krane, K.H., 2020. A convolutional neural network architecture for Sentinel-1 and AMSR2 data fusion. *IEEE Transactions on Geoscience and Remote Sensing*, *59*(3), pp.1890-1902.

OSI SAF Global Sea Ice Concentration (SSMIS), OSI-401-d, doi:10.15770/EUM_SAF_OSI_NRT_2004. EUMETSAT Ocean and Sea Ice Satellite Application Facility. Data extracted from OSI SAF FTP server/ ftp://osisaf.met.no/archive/: (2021/09/04, 2021/09/18, 2021/09/27,) accessed 2025/01/24.

Wang, L., Scott, K.A. and Clausi, D.A., 2016. Improved sea ice concentration estimation through fusing classified SAR imagery and AMSR-E data. *Canadian Journal of Remote Sensing*, *42*(1), pp.41-52.

Wulf, T., Buus-Hinkler, J., Singha, S., Shi, H., & Kreiner, M. B., 2024. Pan-Arctic sea ice concentration from SAR and passive microwave. The Cryosphere, 18(11), pp.5277–5300

https://doi.org/10.5194/ica-abs-10-105-2025